




Long-term humoral immunogenicity, safety and protective efficacy of inactivated vaccine against COVID-19 (CoviVac) in preclinical studies

Liubov I. Kozlovskaya ^{a,b,*}, Anastasia N. Piniava^{a,*}, Georgy M. Ignatyev^{a,*}, Ilya V. Gordeychuk^{a,b,*}, Viktor P. Volok ^{a,c,*}, Yulia V. Rogova^a, Anna A. Shishova^{a,b}, Anastasia A. Kovpak^a, Yury Yu. Ivin^a, Liliya P. Antonova^a, Kirill M. Mefyod^a, Lyubov S. Prokosheva^a, Anna S. Sibirskina^a, Yuliya Yu. Tarasova^a, Ekaterina O. Bayurova^a, Olga S. Gancharova^a, Victoria V. Illarionova^a, Grigory S. Glukhov^c, Olga S. Sokolova^c, Konstantin V. Shaitan^c, Anastasia M. Moysenovich^c, Stanislav A. Gulyaev^a, Tatiana V. Gulyaeva^a, Andrey V. Moroz^a, Larissa V. Gmyl^a, Elena G. Ipatova^a, Mikhail P. Kirpichnikov^c, Alexey M. Egorov^{a,c}, Aleksandra A. Siniugina^a and Aydar A. Ishmukhametov ^{a,b}

^aChumakov Federal Scientific Center for Research and Development of Immune-and-Biological Products of Russian Academy of Sciences, Moscow, Russia; ^bInstitute for Translational Medicine and Biotechnology, Sechenov First Moscow State Medical University, Moscow, Russia; ^cDepartment of Biology, Lomonosov Moscow State University, Moscow, Russia

ABSTRACT

The unprecedented in recent history global COVID-19 pandemic urged the implementation of all existing vaccine platforms to ensure the availability of the vaccines against COVID-19 to every country in the world. Despite the multitude of high-quality papers describing clinical trials of different vaccine products, basic detailed data on general toxicity, reproductive toxicity, immunogenicity, protective efficacy and durability of immune response in animal models are scarce. Here, we developed a β -propiolactone-inactivated whole virion vaccine CoviVac and assessed its safety, protective efficacy, immunogenicity and stability of the immune response in rodents and non-human primates. The vaccine showed no signs of acute/chronic, reproductive, embryo- and fetotoxicity, or teratogenic effects, as well as no allergenic properties in studied animal species. The vaccine induced stable and robust humoral immune response both in form of specific anti-SARS-CoV-2 IgG and NABs in mice, Syrian hamsters, and common marmosets. The NAB levels did not decrease significantly over the course of one year. The course of two immunizations protected Syrian hamsters from severe pneumonia upon intranasal challenge with the live virus. Robustness of the vaccine manufacturing process was demonstrated as well. These data encouraged further evaluation of CoviVac in clinical trials.

ARTICLE HISTORY Received 26 April 2021; Revised 16 August 2021; Accepted 18 August 2021



KEYWORDS Vaccine; SARS-CoV-2; COVID-19; neutralizing antibodies; safety; immunogenicity; inactivated vaccine; preclinical study

Introduction

The ongoing pandemic of coronavirus disease 2019 (COVID-19), which is caused by severe acute respiratory syndrome coronavirus 2 (SARS-CoV-2), has claimed more than four million lives as of March 2021 [1, 2], and the pressure for rapid introduction of safe and effective vaccines against this disease remains very high. The unprecedented in recent history global spread of this pandemic urges the implementation of all existing vaccine platforms to eventually ensure the availability of the vaccines against COVID-19 to every country in the world.

SARS-CoV-2 belongs to subgenus *Sarbecovirus* of genus *Betacoronavirus* of the family *Coronaviridae* [3] and employs the angiotensin-converting enzyme

2 (ACE2) as its main receptor for entering human cells [4, 5]. The enveloped virion of SARS-CoV-2 is 100–150 nm in diameter and is roughly spherical in shape. The virion contains several structural proteins: spike glycoprotein (S), membrane protein (M), envelope protein (E), located on the surface and the nucleocapsid protein (N), which binds to viral RNA inside the particle. The S protein is a type I fusion transmembrane protein, which undergoes extensive glycosylation during synthesis and is cleaved by a host protease into two fragments S1 and S2. The S1 fragment contains the receptor-binding domain (RBD) that interacts with the host cell receptor, ACE2. The S2 fragment is responsible for the membrane fusion after another proteolytic cleavage by host proteases

CONTACT Liubov I. Kozlovskaya  lubov_i_k@mail.ru  Chumakov Federal Scientific Center for Research and Development of Immune-and-Biological Products of Russian Academy of Sciences, Moscow 108819, Russia Institute for Translational Medicine and Biotechnology, Sechenov First Moscow State Medical University, Moscow 127994, Russia

*These authors contributed equally.

 Supplemental data for this article can be accessed at <https://doi.org/10.1080/22221751.2021.1971569>.

© 2021 The Author(s). Published by Informa UK Limited, trading as Taylor & Francis Group.

This is an Open Access article distributed under the terms of the Creative Commons Attribution-NonCommercial License (<http://creativecommons.org/licenses/by-nc/4.0/>), which permits unrestricted non-commercial use, distribution, and reproduction in any medium, provided the original work is properly cited.

and subsequent structural rearrangements [6]. These properties make spike protein and its RBD the main targets of the host neutralizing antibodies (NAbs) [7].

The immune response to SARS-CoV-2 infection has been actively studied in order to produce and improve diagnostics and vaccines. Nab levels have been experimentally shown to be one of the main correlates of protection against SARS-CoV-2, as adoptive transfer of purified IgG from convalescent rhesus macaques protected naive recipient macaques against challenge with SARS-CoV-2 in a dose-dependent manner [8]. Mild-to-moderate course of COVID-19 leads to the development of NAbs, which correlate with anti-RBD IgG measured by ELISA and last at least from two or three [9,10] to five months [11]. Considering the possibility of waning levels of antibodies after the infection, the cellular components of the immunity, which are more difficult to study, are also under close inspection.

Numerous approaches are being tested for the development of vaccines against COVID-19, and currently, the most frequently used are inactivated, viral vector, nucleic acid (RNA, DNA) and protein (subunit, VLP) vaccines [12]. Most vaccines employ the S protein and RBD as the major antigens eliciting NAbs. Different advanced vaccine technologies have already demonstrated their potential in preventing COVID-19, and several such vaccines, including mRNA and adenoviral vector vaccines, have been authorized for use around the globe after successfully completing clinical trials [13,14]. Nevertheless, a more traditional approach, the development of inactivated vaccines, is robust, cost-efficient and reliable due to its long and successful history of use [15,16]. Several inactivated vaccines against SARS-CoV-2 infection are being developed around the world, and at least five have shown success in preclinical and clinical trials, which led to their authorization for use [17–20]. Still, despite the multitude of high-quality papers describing clinical trials of different vaccine products, basic detailed data on general toxicity, reproductive toxicity, protective efficacy, immunogenicity and durability of immune response in animal models are scarce.

In this work, we developed a β -propiolactone-inactivated whole virion vaccine CoviVac and assessed its safety, protective efficacy, immunogenicity and stability of the immune response in rodents and non-human primates. The vaccine showed no signs of acute/chronic, reproductive, embryo- and fetotoxicity or teratogenic effects, as well as no allergenic properties in studied animal species. The vaccine produced stable and robust humoral immune response both in form of specific anti-SARS-CoV-2 IgG and NAbs in BALB/c mice, Syrian hamsters and common marmosets. The Nab levels did not decrease significantly over the course of one year. Protective efficacy of the

vaccine was studied in Syrian hamsters. Robustness of the vaccine manufacturing process was demonstrated by evaluating four batches of the vaccine and comparing their immunogenic properties in mice.

Materials and methods

Cells and viruses

Vero cell line was obtained from Biologicals, World Health Organization, Switzerland.

For laboratory experiments cells were maintained in Dulbecco's Modified Eagle Medium (DMEM, Chumakov FSC R&D IBP RAS, Russia), supplemented with foetal bovine serum (FBS, Gibco, 5%), streptomycin (0.1 mg/ml) and penicillin (100 units/ml) (PanEco, Russia).

For vaccine production cells were maintained in Eagle's MEM (Chumakov FSC R&D IBP RAS, Russia), supplemented with 5% FBS. Cells were expanded in disposable bioreactors (Cytiva, USA and Sartorius AG, Germany) on microcarriers Cytodex1 (Cytiva) at 37°C.

The SARS-CoV-2 vaccine strain AYDAR-1 (GISAID EPI_ISL_428851) was isolated from a nasopharyngeal swab sample of a COVID-19 patient. The virus passage history is described in the Results section. The production virus seeds were stored as infected Vero cell suspension at -196°C .

The SARS-CoV-2 challenge strain PIK35 (GISAID EPI_ISL_428852) was isolated from a nasopharyngeal swab sample of a COVID-19 patient. The virus was passaged 5 times in Vero cells, stored as infected cell suspension at -70°C and used for laboratory experiments and controls. Passages 2, 4, 5 and 6 were sequenced with HiSeq (Illumina, USA). Passages 4–6 acquired a synonymic nucleotide mutation in nsp5 as compared to the primary isolate. No other differences were observed (data not shown).

Vaccine lots

Inactivated purified vaccine against COVID-19 (CoviVac) contains viral antigen ($\geq 3 \mu\text{g}/\text{dose}$), aluminium hydroxide (0.4 mg/dose) and sodium-phosphate buffer saline up to 0.5 ml.

For safety and immunogenicity studies, vaccine lots were prepared with different antigen content: 1.5 $\mu\text{g}/\text{dose}$ (lot InCV-03), 3 $\mu\text{g}/\text{dose}$ (lot InCV-04) and 6 $\mu\text{g}/\text{dose}$ (lot InCV-05) – and placebo vaccine (lot Placebo-InCV-01), containing aluminium hydroxide (0.3–0.5 mg/dose) and phosphate buffer saline up to 0.5 ml.

For assessments of protective efficacy and robustness of the manufacturing process, production lots InCV-04, InCV-12, InCV-14 and InCV-15 with antigen content 3–6 $\mu\text{g}/\text{dose}$ were used.

Visualization of inactivated viral particles with transmission electron microscopy (TEM)

Copper grids (300 mesh formvar/carbon-coated) (Ted Pella) were hydrophilized by glow discharge (−20 mA, 45 s) with the Emitech K100X apparatus (Quorum Technologies, UK). Samples of purified vaccine fractions (3 µl) were placed onto the grid and incubated at room temperature for 30 s. The excess of the sample was removed with filter paper. The grids were stained with 2% aqueous uranyl acetate solution for 30 s at 20°C and air-dried.

Micrographs were acquired using an analytical transmission electron microscope Jem-2100 (JEOL, Japan) equipped with a 2 K × 2 K CCD camera Ultra-scan 1000XP (Gatan, USA). The microscope was operated at 200 kV in a low dose mode, with a magnification of ×40000 (2.5 Å/pix) and a defocus of 0.5–1.9 µm.

SDS-PAGE

Sodium dodecyl sulfate–polyacrylamide gel electrophoresis (SDS–PAGE) was used to separate proteins of purified vaccine preparations. After mixing with SDS–PAGE sample buffer containing SDS and β-mercaptoethanol, samples were heated at 95°C for 5 min and resolved in SDS–polyacrylamide gels with Tris–glycine running buffer, and stained with Coomassie blue.

Western blot

After SDS–PAGE proteins were transferred onto nitrocellulose membranes (BioRad, USA) at 90 V for 1 h. Membranes were then incubated with 30 ml Tris-buffered saline with Tween (TTBS) buffer (pH 8.0) containing 5% nonfat dry milk for 1 h at 20°C. Membranes were stained with a 1:1000 dilution of COVID-19 convalescent serum or rabbit anti-protein S serum (rabbits were immunized twice with 150 µg of recombinant human coronavirus SARS-CoV-2 Spike Glycoprotein (ab273068, Abcam, UK) with three weeks interval and immunoglobulins were purified on HiTrap protein G column (Cytiva) by incubating overnight at 4°C). After washing with TTBS buffer, the membranes were incubated with a secondary antibody (anti-Human or anti-Rabbit IgG (H + L), HRP conjugate, Promega, USA), diluted 1:1000 for 1 h. The membranes were finally washed with TTBS before the Clarity Western substrate (BioRad) was applied, and visualized on films.

Infection and immunostaining of Vero cells

Cells grown on coverslips in 6-well plates were infected with SARS-CoV-2 strain AYDAR-1 and incubated at 37°C for 72 h with subsequent fixation and

inactivation with 3.7% paraformaldehyde in PBS for 30 min. Then cells were successively incubated in 0.2% Triton X-100 in PBS for 5 min at 20°C, 5% dry milk in PBS for 1 h at 20°C, anti-SARS CoV-2 serum (human convalescent serum or immunized mouse serum) diluted in 5% dry milk in PBS with 0.05% Tween-20 for 2 h at 37°C, secondary FITC-conjugated antibodies (anti-Human or anti-Mouse, Sigma) for 1 h at 37°C, and with 1 µg/ml Hoechst 33342 (Sigma, USA) in ddH₂O for 15 min at 20°C. After each step, cells were washed thrice with PBS. The coverslips were placed onto a drop of 10% Mowiol in 0.1M Tris-HCl pH 8.5. Images were captured on an Eclipse Ti-E microscope with the A1 confocal module (Nikon Corporation, Japan) and the objective Apo TIRF Plan Fluor 63 × 1.49. At least 50 infected cells in 10 distinct fields were analysed.

ELISA

ELISA was performed using kits for the determination of IgG to SARS-CoV-2 N protein and partial spike (S) protein (Lytech, Russia, prepared for laboratory use only), and total antibodies to RBD (SARS-CoV-2-CoronaPass, NextGen, Russia), according to the manufacturer's protocol.

Virus neutralization test (NT)

Eight two-fold serum dilutions were prepared in DMEM (Chumakov FSC R&D IBP RAS, Russia). The dilutions were mixed with equal volumes of virus suspension (strain PIK35 SARS-CoV-2) containing 50–200 TCID₅₀ per well. Final serum dilution series started from 1:8. After 1 h incubation at 37°C, virus-serum mixtures were added to the confluent Vero cell monolayers in 2 replicates. In parallel with every test run, control cells were incubated with the analogous sequential dilutions of non-immune and standard immune control sera; and a virus dose titration was performed. After a 5-day incubation at 37°C, cytopathic effect (CPE) was visually assessed via a light microscope. Antibody titers were calculated according to the Karber method [21]. The result of <1:8 was considered negative.

Ethical approval

The animal study protocols were approved by the Ethics Committee of the Chumakov FSC R&D IBP RAS (#140720-1 from 14 July 2020) and by Bioethics Committee of RMC “Home of pharmacy” (#3.50/20 and #4.50/20 from 2 September 2020). Animals were maintained in accordance with the Directive of the European Parliament and of the Council 2010/63/EU dated 22 September 2010 on the protection of animals used for scientific purposes and the Sanitary Rules for the design and maintenance of experimental biological clinics in the Russian Federation (1045-73).

Animal models for safety studies

Detailed experimental procedures are presented in the Results section and Supplementary information.

Outbred ICR (CD-1), inbred BALB/c (haplotype H-2d) mice, males and females distributed equally, 18–22 g (8–10 weeks old), were purchased from Scientific Center of Biomedical Technologies, branches Andreevka or Stolbovaya, Russia. For safety, sensitivity and immunogenicity studies, mice were randomized by weight between groups. Inoculations were performed: with 0.5 ml vaccine or placebo intramuscularly (IM) in the upper third of all four limbs, intravenously (IV) in the tail vein, or subcutaneously (SC). Mice were observed daily. Blood samples were collected *intra vitam* from the facial vein.

Guinea pigs, males and females distributed equally, 350–450 g (12–16 weeks old), were purchased from Scientific Center of Biomedical Technologies, branch Andreevka, Russia. For safety and sensitization studies, animals were randomized by weight between groups and inoculated with 0.5 ml vaccine or placebo through IM or SC routes. Animals were observed daily. Blood was sampled *intra vitam* from the lateral saphenous vein.

Outbred Syrian hamsters, males and females distributed equally, 35–45 g (3–4 weeks old) were purchased from Scientific Center of Biomedical Technologies, branch Stolbovaya, Russia. For immunogenicity studies, animals were randomized by weight between groups and inoculated with 0.5 ml vaccine or placebo through IM route (in the upper third of the hind limb) twice with a 14-days interval. Blood was sampled from the lateral saphenous vein weekly.

Outbred Wistar rats, pregnant females, 180–250 g, 9–12 weeks old, bred and maintained by RMC “Home of pharmacy,” were inoculated IM with 0.5 ml. Dams, and later the offspring, were observed daily and weighed every 3 days.

Outbred Wistar rats, females (199–286 g) and males (215–344 g), 9–12 weeks old, bred and maintained by RMC “Home of pharmacy,” were immunized IM multiple times with a 0.5–1.0 ml vaccine or placebo per injection. Animals were allowed to mate on days 29–42, half of dams were observed till days 20–21 of pregnancy and other half till the time of labour and delivery. The offspring was observed for 45 days.

Common marmosets (*Callithrix jacchus*), males and females, 360–400 g (2–5 years old), were bred and maintained in the Experimental Clinic of Callitrichidae at the Chumakov FSC R&D IBP RAS. The conditions of housing and maintenance of the animals remained unchanged throughout the experiment. All animals were identified using subcutaneous radio-frequency chips with unique 15-digit codes (Globalvet, Moscow, Russia). The IDs in tables and figures represent the last four digits of the code. During the safety and immunogenicity studies, marmosets were IM inoculated with

0.5 ml of the vaccine or placebo (0.25 ml into a thigh muscle of each leg). Venous blood samples (up to 2 ml) were obtained by femoral vein puncture.

Protective efficacy study in Syrian hamsters

Outbred Syrian hamsters, males and females distributed equally, 35–45 g (3–4 weeks old) were purchased from Scientific Center of Biomedical Technologies, branch Stolbovaya, Russia. Animals were randomized by weight between groups: intact ($N = 5$), unvaccinated control ($N = 15$) and vaccinated ($N = 15$). Vaccinated group was inoculated with 0.5 ml vaccine (5 µg/dose) through IM route (in the upper third of the hind limb) twice with a 14-days interval. Vaccinated and unvaccinated hamsters were infected intranasally with 10^5 TCID₅₀ (25 µl into each nostril) with SARS-CoV-2 strain PIK35 14 days after the 2nd immunization. Animals were observed and weighed daily, nasal and rectal swabs were collected. Five animals from each group were euthanized on days 4, 7 and 14 post infection (p.i.). Lungs, brain, liver, kidney, spleen and heart tissues were collected for investigation. Organs were homogenized in physiological saline using TissueLyser (Qiagen, USA). Swabs and organ suspensions were examined for the presence of viral RNA by POLYVIR SARS-CoV-2 (Lytech, Russia) according to the manufacturer’s protocol.

Histological examination

Organs for histopathological examination were fixed in 10% neutral buffered formalin for 48 h at room temperature, dehydrated in isopropyl alcohol and embedded in paraffin medium. Formalin-fixed paraffin embedded (FFPE) tissue blocks with lungs were used to obtain 3 micrometer-thick cross-sections from all lung lobes (2 sections for each tissue block). Lung sections were stained with haematoxylin and eosin and examined using Zeiss Axio Observer A1 microscope (Carl Zeiss, Germany). Microphotographs were obtained by Digital Microscopy Camera Axio-Cam 305 (Carl Zeiss) and processed using Zen Blue Edition (Carl Zeiss) and Photoshop CS6 software (Adobe, USA). Semi-quantitative pathological assessment was performed on tissue slides. The semi-quantitative morphological scores of pneumonia (4–7 d p.i.) or post-pneumonia changes (14 d p.i.) were calculated using 5-grade system (0–4), where 0 – no pneumonia changes, 1 – mild changes, 2 – moderate changes, 3 – severe changes, 4 – extra severe changes.

Blood analysis

Leukocyte formula was calculated in dry, fixed blood smears stained with May-Grunwald’s eosin-methylene

blue and azure-eosin by Romanovsky (Abris, Russia), according to the manufacturer's instructions.

Biochemical analysis of animal blood sera was carried out using an automated biochemical analyzer Cobas C111 (Roche, Switzerland).

Splenocyte proliferation assay

BALB/c mice were randomized by weight between groups and immunized twice with the vaccine with 6 µg/dose (0.5 ml) or PBS with a 14-day interval. Groups of mice were euthanized on days 0, 7, 14 and 21 after the 1st immunization. Spleens were collected under aseptic conditions, gently grinded in RPMI-1640 medium (Gibco, USA), cleared from cell debris by a short spin (20 s, 400 g), and the cells were pelleted by centrifugation (5 min, 400 g). Cells were further resuspended in erythrocyte lysis buffer (0.02 M Tris-HCl, 0.15 M NH₄Cl, pH 7.2) and incubated at room temperature for 5 min. Then, splenocytes were washed twice with RPMI-1640 (5 min, 400 g). Afterward, the pellet was resuspended in complete growth medium (RPMI-1640 medium, 5% foetal bovine serum (ICN, USA), 2 mM L-glutamine (ICN), 20 mM HEPES (Sigma, USA), 100 U/ml penicillin and 100 µg/ml streptomycin). Cells were stained with 0.4% trypan blue solution (Flow Laboratories, USA) and the proportion of viable cells was determined. Splenocytes (10⁵ cells/well) were seeded in 96-well plates in complete growth medium. Mitogens concanavalin A (ConA, ICN) and lipopolysaccharide (LPS) from *S. typhimurium* (Sigma) were used as positive control mitogens. Inactivated SARS-CoV-2 and Chikungunya virus in concentration 5 µg/ml were used as specific and non-specific antigens, correspondingly. Both viral antigens were prepared from the virus propagated in Vero cells, inactivated by β-propiolactone and chromatographically purified as described in the Results. Control cells were left intact without stimulation in the same volume of media. Cells were incubated for 96 h at 37°C with 5% CO₂.

Splenocyte proliferation was assessed in tetrazoline/formazan assay [22]. In brief, XTT:PMS (4:1) (Sigma) solution was added to the wells 8 h before the end of the incubation period. Optical density was recorded at 450 nm against a control wavelength of 630 nm. The test result was calculated as a stimulation index: $IS = OD_{stim} / OD_{control}$, where IS – stimulation index, OD_{stim} – optical density in the well with stimulated splenocytes, OD_{control} – optical density in control wells. All experiments were carried out in duplicates.

Statistical analysis

Statistical assessment of the differences in the studied parameters of general animal wellbeing, biochemical

and hepatological analysis in experiments with non-human primates was performed using 2-way ANOVA with the Gressier-Greenhouse correction followed by Šidák multiple comparisons test in Prism 8 (v. 8.4.2, GraphPad, USA).

Statistical analysis of the differences in the studied parameters of antibody titers, Ct values, weights etc. in protectivity assessment studies was performed using Mann–Whitney test. Comparisons and visualizations were performed in OriginPro 8 (OriginLab, USA).

The figure legends and Methods denote the number of animals in each group and specific details on statistical tests.

Results

Vaccine production and description

The vaccine strain AYDAR-1 isolation and genetical description was presented previously [23]. The virus on the 3rd passage was filtered and further purified by dilution. The primary, master and working seed lots of the strain were established (namely, passages 7, 8 and 9) and characterized following the national guidelines for vaccine production. All three seed lots (primary, master and working) were analysed using HiSeq (Illumina). No mutations (SNVs over 1%) were found compared to the original isolate (data not shown).

The vaccine production process (Figure 1(A)) starts with the virus propagation in Vero cells on microcarriers, followed by β-propiolactone inactivation (1:1000–1:2000 (v/v)) at 4°C for 24–48 h, ultrafiltration, diafiltration, chromatographic purification and sterilizing filtration. Concentrates are tested for completeness of inactivation upon three consecutive passages of the inactivated material in Vero cells followed by immunofluorescence staining of the infected cells with anti-SARS-CoV-2 antibodies revealed with FITC-conjugated antiserum.

Finally, the vaccine is diluted with phosphate buffer saline and supplemented with aluminium hydroxide gel. Sterility, total protein concentration, residual DNA, residual β-propiolactone, endotoxins and other parameters are controlled in the concentrates or the final vaccine lot.

Transmission electron microscopy (TEM) (Figure 1(B)) of negatively stained concentrates revealed pleomorphic spherical particles about 120 nm in diameter covered with spike-like structures, 16–20 nm in length.

SDS-PAGE and Western blot (WB) of the vaccine concentrates before inactivation and after chromatography stained with COVID-19 convalescent sera (Figure 1(C,D)) revealed two main proteins in the concentrates: N and S, which is expected for a whole virion preparation. Staining with an anti-S protein serum (Figure 1(E)) revealed the presence of two

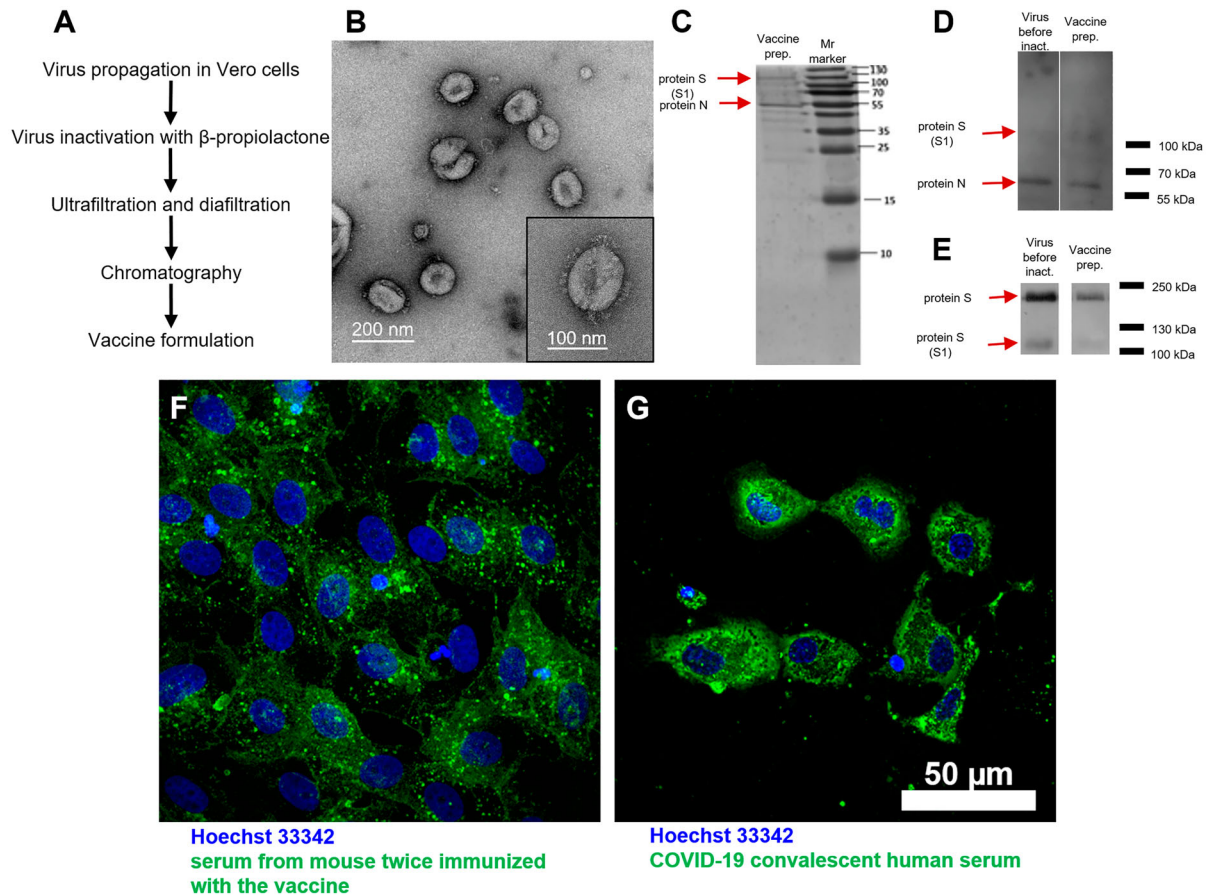


Figure 1. CoviVac vaccine production process and identity testing: (A) Principal structure of the vaccine production process. (B) TEM of the negatively stained inactivated vaccine concentrate after chromatographic purification; representative particle (bottom right). (C) SDS-PAGE of the vaccine preparation (purified inactivated virus preparation after chromatography), stained with Coomassie blue. (D) Western blot of the virus preparation before inactivation and vaccine preparation (purified inactivated virus preparation after chromatography), stained with COVID-19 convalescent human serum. (E) Western blot of the virus preparation before inactivation and vaccine preparation (purified inactivated virus preparation after chromatography), stained with anti-S protein rabbit serum. (F) Vero cells infected with SARS-CoV-2 and stained with serum of a CoviVac-immunized mouse (green) and Hoechst 33342 (blue). (G) Vero cells infected with SARS-CoV-2 and stained with COVID-19 convalescent human serum (green) and Hoechst 33342 (blue)

forms of the S protein in the virus preparations before and after inactivation: S1 and a full-length S protein. This finding signifies that the target antigen for the induction of NABs is present in the vaccine preparation.

Immunofluorescent staining of SARS-CoV-2 infected Vero cells with sera from the vaccine-immunized mice and COVID-19 convalescent serum (Figure 1(F,G), correspondingly) revealed virus antigens localized to the cell cytoplasm and intracellular inclusions. Immunofluorescence staining confirmed the reactivity of vaccine-induced antibodies with viral antigens in the infected Vero cells.

Safety in mice and Guinea pigs

Safety experiments were performed using the high dose of vaccine antigen (6 µg/dose, 0.5 ml).

For acute toxicity study outbred mice ($N = 25$) and guinea pigs ($N = 20$) were inoculated with vaccine IM

or IV (formulation without aluminium hydroxide, 6 µg/dose, 0.5 ml). Control mice ($N = 25$) and guinea pigs ($N = 20$) were inoculated with placebo formulation IM or physiological saline IV (0.5 ml). Animals were observed for 7 days for mortality, weight change, general condition, behavioural reactions and neurological status (Supplementary Tables S1–3). Mice and guinea pigs in all groups gained body weight. The condition and behaviour of the experimental animals were normal and did not differ from the control animals during the whole period of observation. An autopsy did not reveal any pathological changes or differences between vaccinated and control groups.

For chronic toxicity study outbred mice ($N = 20$) and guinea pigs ($N = 20$) were daily inoculated IM with the vaccine for 10 days. Control mice ($N = 20$) and guinea pigs ($N = 20$) were analogously inoculated with placebo formulation (0.5 ml). Animals were observed for 7 days after the last inoculation for

mortality, weight changes, general condition, behavioural reactions, and neurological status. Half of the animals in each group were euthanized on day 1 and the other half on day 8 after the last injection for histological examination. There were no observable changes in the clinical condition, behaviour or weight gain of vaccinated and control animals (Supplementary Tables S4–6). Blood analysis of animal sera sampled at the end of the observation period did not reveal any abnormal changes in tested biochemical parameters (Supplementary Table S7). An autopsy did not reveal any pathological changes or differences between vaccinated and control groups.

For immediate hypersensitivity study, guinea pigs ($N=30$) were sensitized by SC inoculation with a single dose of the vaccine and with another IM dose administered the next day. Negative control animals were inoculated with 0.5 ml of phosphate buffer saline at the same time points. Positive control animals were sensitized with heterologous horse serum (Biolot, Russia). After 14 days, animals in each group were inoculated IV with the same dose of the preparation used for sensitization (vaccine, phosphate buffer saline or horse serum, correspondingly). After the stimulation, animals were observed for anaphylactic reactions for 30 min. Positive control animals showed pronounced signs of anaphylaxis, while experimental and negative control animals showed some scratching without any other abnormal signs (data not shown).

Delayed-type hypersensitivity was assessed in BALB/c mice ($N=20$). The mice were inoculated IP with the vaccine. Control animals were inoculated with phosphate buffer saline. After 19 days, animals were challenged SC with the vaccine (formulation without aluminium hydroxide) in one hind leg and phosphate buffer saline in the other. On day 20, the respective legs (foot pads) were compared by weight (Supplementary Table S8). The vaccine did not cause an inflammatory reaction when administered to animals not sensitized by the vaccine. Conversely, when animals were sensitized, oedema development was observed, signifying a specific reaction to the vaccine antigen.

For assessment of the indirect sensitizing effect of the vaccine on preexisting immunity to ovalbumin, BALB/c mice ($N=60$) were immunized SC with ovalbumin (0.5 µg, Sigma, in aluminium hydroxide, 0.5 ml) twice, and 10 days later half of the animals were immunized IM with the vaccine. On days 10, 17 and 21 after the first immunization blood samples were collected, pooled and studied for the presence of antibodies to ovalbumin in ELISA. Antibody titers to ovalbumin did not differ between experimental and control groups on days 7 and 14 (Supplementary Table S9) and did not decrease after immunization with the vaccine.

Therefore, the vaccine CoviVac did not show signs of acute or chronic toxicity, immediate

hypersensitivity and did not suppress the humoral immunity to a heterogeneous antigen in studied animal models.

Safety in non-human primates (*Callithrix jacchus*)

Common marmosets were IM vaccinated twice with a 14-day interval: 2 males and 4 females were immunized with the high dose (6 µg/dose, 0.5 ml), 1 male received a medium dose (3 µg/dose, 0.5 ml), and 1 female and 2 males were inoculated with the placebo (0.5 ml). General condition of the animals was observed daily. Body mass and temperature were monitored twice a week. Blood samples were collected on days 0, 7, 14, 21 and 28 after the first immunization and complete blood cell count (CBC) and biochemical analysis (ALT, AST, protein, albumin, urea, creatinine, amylase, bilirubin, C-reactive protein) were performed. No significant differences were observed between experimental and control animals by these parameters (Supplementary Tables S20–23).

Therefore, the vaccine CoviVac was considered safe for non-human primates (*Callithrix jacchus*).

Study of embryo-, fetotoxicity and teratogenic effects in the antenatal and postnatal periods of development

Pregnant Wistar rats ($N=60$) were randomized to 3 groups and immunized IM on days 2, 9, and 16 of pregnancy. The first study group was immunized with one dose of the vaccine (6 µg/dose, 0.5 ml), second study group with double dose (12 µg/dose, 1.0 ml) and third control group with double dose of the placebo vaccine (1.0 ml). Body weight and general physical condition of animals was assessed daily; in the late stage of pregnancy, exploratory activity and dams were assessed in the open field test (Supplementary Tables S10–11). Dams gained weight normally; no deaths or signs of intoxication were observed. Signs of premature or difficult labour were not observed in any of the study groups. In the open field test on day 18 of pregnancy all female rats demonstrated a predominantly balanced type of behaviour with moderate motor and search activity without signs of anxiety.

Half ($N=10$ per group) of animals in each group were euthanized on day 20 of pregnancy. There were no statistically significant differences between the groups in the numbers of corpora lutea in the ovaries, implantation sites in the uterus, live and dead foetuses (Supplementary Table S12). Foetuses were normally formed, the topography of all investigated organs was within the limits of the anatomical norm, their histological structure corresponded to the age of the

embryos, bone development was normal. No pathological changes in organs and tissues were found.

The other half ($N = 10$ per group) of the animals from each of the three vaccinated groups were used to identify possible violations of embryonic development manifested in the postnatal period. The offspring was observed for 60 days after birth. The general condition of the rat offspring, survival rate, weight gain (Supplementary Table S13), physical development, maturation of sensory-motor reflexes, emotional-motor behaviour and the ability to finely coordinate movements were assessed (data not shown). The ratio of males and females in the offspring in all groups was almost identical (approximately 1:1). The mortality rate of the offspring for the entire observation period (from birth to two months of age) in all groups did not exceed 4% and did not differ significantly between groups. Physical and neurological development of the rat offspring did not differ between the study groups, and individual values of the studied parameters were within the physiological norm.

Therefore, the vaccine CoviVac had no negative effect on the general condition of pregnant rats. No embryotoxic, fetotoxic or teratogenic effects were discovered. Vaccination did not cause an increase in the mortality rate of the offspring and did not affect the physical and psychological development of the offspring.

Study of reproductive toxicity

Outbred Wistar rats, females ($N = 80$) and males ($N = 40$) were immunized IM multiple times (males were vaccinated 5 times on days 1, 8, 15, 22 and 28; females were vaccinated 3 times on days 14, 21 and 28) with a single ($6 \mu\text{g}/\text{dose}$ in 0.5 ml) or double ($12 \mu\text{g}/\text{dose}$ in 1.0 ml) doses per injection (detailed scheme in Supplementary Table S14). Rats were observed daily and weighed on days of manipulations. No signs of intoxication were observed: body weight (Supplementary Table S15–16), general condition, activity and reaction to stimuli were normal, without signs of depression, excitement or aggression; muscle tone was moderate in all animals, and no coordination disorders were observed. Animals were caged together for mating on days 29–42. There were no differences in the concentration and percentage of motile and non-motile spermatozoa, as well as in the percentage of live, dead and immature spermatozoa after mating in experimental and control groups (data not shown).

Ninety percent of female rats became pregnant after mating in all study groups. Half of the dams in all three groups were euthanized on days 20–21 and other half until the time of labour and delivery. The numbers of implantation sites in uterus, and live and dead fetuses did not differ between experimental and control groups (Supplementary Tables S17–18). Such parameters as weight gain, emotional-motor

behaviour in open field test, morphology and microscopic structure of the organs of dams were within the normal range and did not differ between study groups (data not shown). The average number of live pups in litters, total number of offspring and female/male ratio did not differ between study groups. The ratio of males and females in the offspring was almost identical (approximately 1:1). The mortality rate of the offspring from birth till 1.5 months of age in all groups did not exceed 3.6% (Supplementary Table S19).

Physical development of the offspring was assessed by measuring body weight dynamics, and the timing of the manifestation of physical signs such as detachment of the auricle, the appearance of primary hair, the eruption of incisors, the opening of the eyes, the onset of puberty (drooping of testes in males or opening of vagina in females). In addition, we assessed the rate of maturation of sensory-motor reflexes, emotional-motor behaviour and the ability to finely coordinate the movements up to day 45 after birth (data not shown). None of the studied parameters exceeded the physiological norm and did not significantly differ between the study groups ($p > 0.05$).

Therefore, multiple IM administration of the vaccine CoviVac to male and female rats did not have a negative effect on the reproductive functions of animals and did not affect the development of the offspring.

Immunogenicity in laboratory animals

BALB/c mice ($N = 20$), Syrian hamsters ($N = 15$) and common marmosets ($N = 6$, as used in safety studies) were immunized IM with the vaccine CoviVac ($5\text{--}6 \mu\text{g}/\text{dose}$, 0.5 ml) twice with a 14-day interval. Blood samples were collected every seven days and individually analysed in neutralization test (NT) for NABs against SARS-CoV-2. By day 14, before the 2nd immunization, 40% of mice, 87% of hamsters and 83% of marmosets developed NABs (Figure 2). All immunized animals showed NAB response after two doses of the vaccine, and titers were growing from day 14 to day 28. Two weeks after the 2nd immunization (day 28) 100% of animals had NABs with geometric mean titer (GMT) (\log_2) 6.55 ± 1.01 (BALB/c mice), 8.53 ± 1.34 (hamsters), and 6.84 ± 0.40 (marmosets). Therefore, we observed 100% seroconversion rate with NAB titers over 1:90 after two doses of the vaccine. Interestingly, Syrian hamsters showed the highest seroconversion after a single immunization and the highest NAB titers after two doses of the vaccine.

Antibody specificity after immunization in BALB/c mice

BALB/c mice were randomized by weight ($N = 20$, blood was collected from 10 animals on each time point) and IM inoculated with vaccines with different

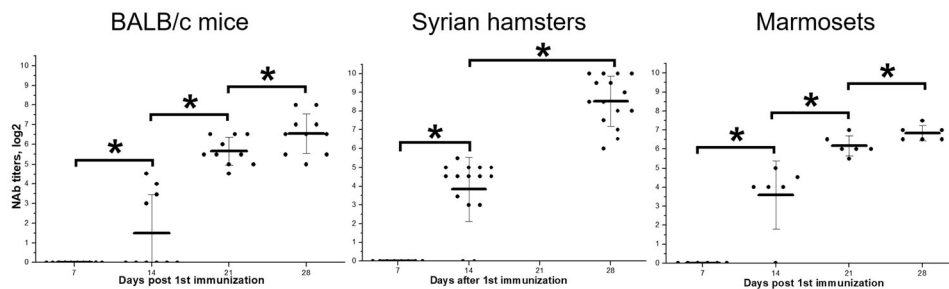


Figure 2. Neutralizing antibody titers against SARS-CoV-2 in BALB/c mice ($N = 20$, blood was collected from 10 animals at each time point), Syrian hamsters ($N = 15$) and marmosets ($N = 6$) vaccinated with CoviVac (lot InCV-05, 6 $\mu\text{g}/\text{dose}$, twice with a 14-day interval). Line shows Mean, whiskers show \pm SD. *Differences are statistically significant (Mann–Whitney test, $p < 0.05$).

antigen content (1.5, 3, and 6 μg per dose, 0.5 ml) or placebo (0.5 ml) twice with a 14-day interval. Blood samples were collected on days 0, 7, 14, 21, and 28 after the 1st immunization and studied in ELISA (in pools) and individually in NT for the presence of specific antibodies against SARS-CoV-2.

NABs (Figure 3(A)) were detected on day 7 after the 1st immunization in 1 out of 10 mice immunized with 3 μg of vaccine antigen. On day 14, detectable NAB titers ($>1:8$) were observed in 4 out of 10 animals in each dose group. On day 21, NABs were detected in all immunized mice. At the same time, NAB GMTs increased during the observation, reaching the maximum levels on day 28. The NAB GMT on days 14, 21 and 28 did not differ significantly between the groups immunized with different doses.

Antibodies to different regions of the S protein (RBD and partial S) were detected in sera of immunized mice on days 7–28 (Figure 3(B)): to S – starting from day 7 in 6 $\mu\text{g}/\text{dose}$ group, to RBD – from day 21. On days 21 and 28, no differences were found between the titers of antibodies to S and RBD in all three dose groups. Antibodies to nucleoprotein N of SARS-CoV-2 were detected on day 21 in all experimental animals but decreased by day 28. Therefore, vaccine-induced anti-SARS-CoV-2 antibodies reached detectable levels on day 14 after the 1st immunization with all tested doses, but NAB titers were seen only in 40% of animals. After the second immunization, on day 21, antibody titers in all animals increased sharply with 100% seroconversion.

Splenocyte proliferation assay

The effect of vaccination on the functional state of spleen lymphocytes (splenocytes) and the formation of a specific cellular response to antigen stimulation was assessed in the splenocyte proliferation assay. BALB/c mice were immunized twice with the vaccine (6 $\mu\text{g}/\text{dose}$, 0.5 ml) or PBS with a 14-day interval. Groups of mice were euthanized at days 0, 7, 14 and 21 after the 1st immunization and used for splenocytes isolation.

The viral antigens used for stimulation (inactivated SARS-CoV-2 and Chikungunya virus) did not suppress the splenocyte proliferation in vitro (day 0 in

all groups) and did not induce a pronounced proliferation of splenocytes of intact animals (Figure 3(C)). The proliferative response of splenocytes to stimulation with mitogens, which were used as a positive control (concanavalin A and lipopolysaccharide), was very pronounced and significantly higher than with viral antigens ($P < 0.001$).

Splenocytes of mice immunized with the vaccine responded to in vitro stimulation with a specific antigen, starting from day 7 (Figure 4). On day 14 after a single vaccination, the stimulation index was higher in comparison with earlier time points. On day 21, in all vaccinated mice the stimulation index for the SARS-CoV-2 antigen significantly exceeded the values seen on day 14 ($P < 0.05$), while neither the stimulation of these cells with heterologous antigen nor the stimulation of cells from non-immunized mice resulted in noticeable proliferation. The effected correlates with the antibody response induction (Figure 3(A,B)). This indicates that vaccination of mice with CoviVac vaccine resulted in the formation of population of SARS-CoV-2-specific lymphocytes.

Protective efficacy study in Syrian hamsters

Syrian hamsters were randomized by weight into three groups: intact ($N = 5$), vaccinated ($N = 15$) and unvaccinated control ($n = 15$). Vaccinated group animals were IM inoculated with vaccine (5 μg per dose, 0.5 ml) twice with a 14-day interval (data on NAB titers are presented and discussed in Figure 2) and intranasally challenged 14 days after the 2nd immunization with 10^5 TCID₅₀ of SARS-CoV-2 strain PIK35. All animals were observed and weighted daily, nasal and rectal swabs were collected. Five animals from experimental groups were euthanized on days 4, 7 and 14 post infection (p.i.). Intact animals were euthanized on day 14 p.i. Lungs and visceral organs were collected for RT-PCR and histological investigation. The data are presented in Figure 4.

No mortality was observed in all groups throughout the challenge experiment.

Intact group animals gained weight during the observation period (Figure 4(A)). Unvaccinated

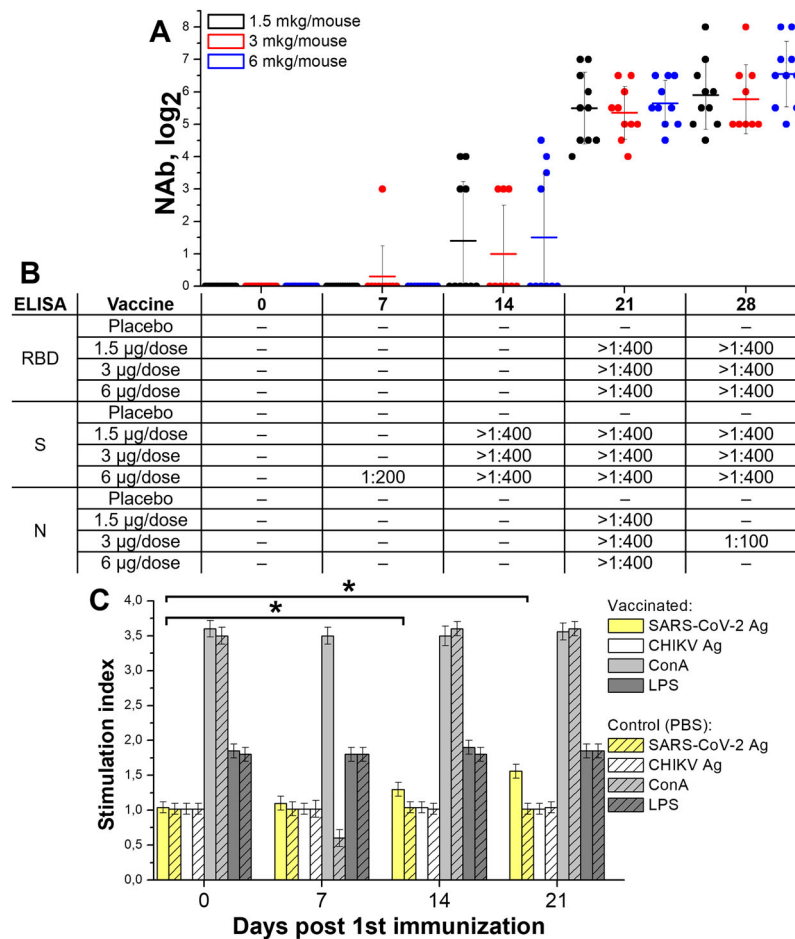


Figure 3. Immune response in BALB/c mice ($N = 20$ /group, blood was collected from 10 animals/group on each time point) immunized with three doses of the vaccine CoviVac (1.5, 3, and 6 µg per dose, twice with 14-day interval). Samples were collected and investigated on days 7, 14, 21 and 28 post 1st immunization. (A) Neutralizing antibody titers in mice of each group. Line shows Mean, whiskers show \pm SD. (B) Antibody response against SARS-CoV-2 proteins (N, S and RBD) in ELISA. Serum samples from each group were studied in pools. (C) Splenocyte proliferation assay (6 µg per dose, twice with a 14-day interval). [SARS-CoV-2 - inactivated SARS-CoV-2 (0.5 µg/well); CHIKV - inactivated Chikungunya virus (0.5 µg/well); ConA - Concanavalin A (0.5 µg/well), LPS - lipopolysaccharide of *S. typhimurium* (0.5 µg/well)] *Stimulation index differences from day 0 are significant (t -test, $p < 0.001$)

control animals lost weight until day 6 p.i. Vaccinated animals lost some weight on day 1 p.i., but starting from day 2 p.i. gained weight, and weighed more in comparison with the control group (Mann–Whitney test, $p < 0.05$). On day 5 p.i. the difference in weight between intact and vaccinated animals was statistically insignificant (Mann–Whitney test, $p > 0.05$).

Nasal and rectal swabs from five hamsters from each experimental group were analysed for SARS-CoV-2 RNA daily (Figure 4(B,C)). Ct values in RT–PCR for viral RNA were significantly higher and the numbers of viral RNA-positive animals were significantly lower in vaccinated group from day 1 p.i. On days 7–10 p.i. all vaccinated animals cleared of viral RNA in nasal swabs. Viral RNA content in rectal swabs increased in both experimental groups from day 1 to day 2 p.i., which signified viral reproduction in infected animals. However, it decreased rapidly in vaccinated animal swabs; and starting from day 3 p.i. most of the vaccinated animals' swabs did not contain viral RNA.

The histopathological examination revealed subacute inflammation in lung lobes by the 4th day in all infected animals examined. In the control group chronic interstitial inflammation, foci of tissue damage and disappearance of the alveolar structure in the lungs developed in the direction from the main bronchus to the subpleural areas (Figure 5). The most severe inflammation with large immunocyte infiltrates was observed on the 7th day in all the examined animals. The proliferative phase of pneumonia on day 7 p.i. affected up to 75 percent of the area of the sections of the lobes of the lungs. These inflammatory changes led to the appearance of mild perivascular fibrosis by 14 d p.i. By day 14 p.i. no severe immunocyte infiltration was detected, and thickening of the alveolar walls was noticeable in the previously affected areas. Only mild changes were observed in the lungs of all vaccinated hamsters at 4–14 d p.i. (Figure 5). On day 7, when the most severe inflammation was observed in the control group, the vaccinated animals showed extremely small foci of

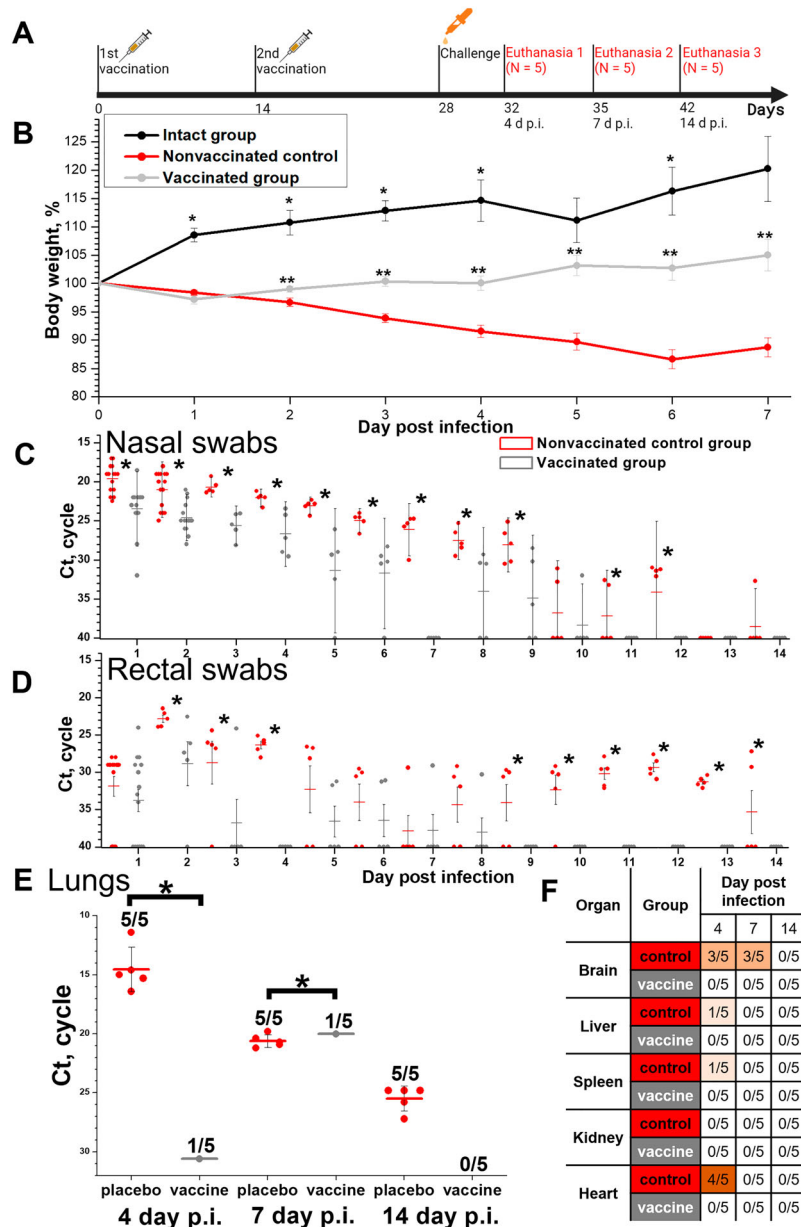


Figure 4. Protective efficacy in Syrian hamsters ($N = 15$, 5 animals were euthanized on days 4, 7 and 14 p.i.) of the CoviVac vaccine (6 μg per dose, 2 immunizations with a 14-day interval) against intranasal challenge 14 days after the 2nd immunization with 10^5 TCID₅₀ of SARS-CoV-2 strain PIK35. (A) Scheme of the experiment (visualized by BioRender). (B) Body weights of intact hamsters and challenged vaccinated and control groups. *Differences between intact and vaccinated groups are statistically significant (Mann–Whitney, $p < 0.05$) **Differences between vaccinated and control groups are statistically significant (Mann–Whitney, $p < 0.05$). (C) Viral RNA presence in nasal swabs of challenged vaccinated and control hamsters on days 1–14 post infection. Line shows Mean, whiskers show \pm SD. *Differences between control and vaccinated groups are statistically significant (Mann–Whitney test, $p < 0.05$). (D) Viral RNA presence in rectal swabs of challenged vaccinated and control hamsters on days 1–14 post infection. Line shows Mean, whiskers show \pm SD. *Differences between control and vaccinated groups are statistically significant (Mann–Whitney test, $p < 0.05$). (E) Viral RNA presence in lungs of challenged vaccinated and control hamsters, collected on days 4, 7 and 14 post infection. Line shows Mean, whiskers show \pm SD. *Differences between control and vaccinated groups are statistically significant (Mann–Whitney test, $p < 0.05$). (F) Viral RNA presence in visceral organs of challenged vaccinated and control hamsters, collected on days 4, 7 and 14 post infection. Numbers signify the number of positive RNA detections per total number of euthanized animals.

tissue damage and a low level of immunocyte infiltration, with complete absence of the proliferative phase of pneumonia. In general, thickening of the walls of the alveoli was the most pronounced sign of the disease in the lungs, which indicated a mild course of the disease in vaccinated animals. Semiquantitative histopathological assessment on lung sections revealed that average pneumonia intensity score on days 4 and 7 in

non-vaccinated control animals was 3, while in vaccinated animals it was 0.8 (Mann–Whitney, $p < 0.05$).

Viral RNA was detected in the lungs of all control group animals (5 of 5) on days 4, 7 and 14 p.i. (Figure 4(D)). The RNA load was decreasing from day 4 to day 14 p.i. Viral RNA was detected on days 4 and 7 p.i. in 1 of 5 vaccinated animals (Figure 4(D)), and was not detected on day 14 p.i.

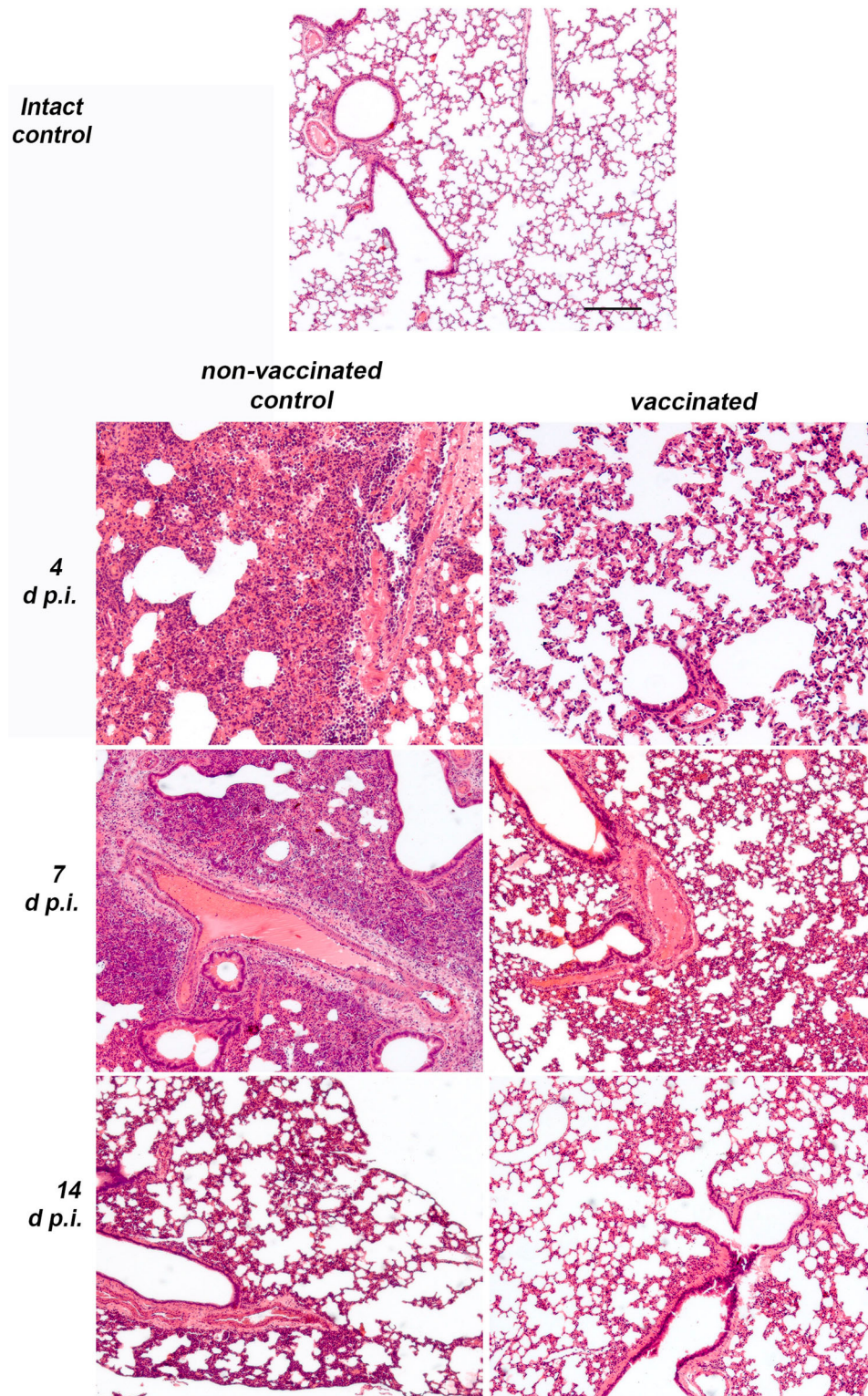


Figure 5. Histopathological findings in non-vaccinated control and vaccinated (6 μg per dose, 2 immunizations with a 14-day interval) Syrian hamsters ($N = 15$ per group, 5 animals were euthanized on days 4, 7 and 14 p.i.) intranasally challenged 14 days after the 2nd immunization with 10^5 TCID₅₀ of SARS-CoV-2 strain PIK35. Representative pathological findings in the lungs of infected hamsters on days 4, 7 and 14 p.i. Haematoxylin and eosin.

Viral RNA was detected in visceral organs of control unvaccinated animals only (Figure 4(E)) and mostly on day 4 p.i. Viral RNA was found in the brain (3 of 5 animals) and heart (4 of 5 animals) specimens collected from unvaccinated animals on day 4 p.i. No viral RNA was detected in the visceral organs of the vaccinated animals.

Dose-dependence and durability of NAb response in mice and marmosets

Three groups of BALB/c mice ($N = 20$ per group) that were twice vaccinated with 1.5, 3, and 6 μg per dose of the vaccine (0.5 ml), respectively, and two groups of marmosets (vaccinated with 3 and 6 μg doses in

0.5 ml, as used in safety studies), which were used for immunogenicity assessment, were left for continued monitoring of NAb titers against SARS-CoV-2. Blood samples were collected every 1–4 weeks and analysed individually in NT (Figure 6). As was shown previously, we observed an increase in NAb titers up to 4 weeks after the 1st immunization (i.e. 2 weeks after the 2nd immunization). For the next almost 50 weeks NAb titers remained at the same level, the differences were not significant ($p > 0.05$) in both mice and marmosets. After week 28 we observed some tendency to decrease in titers, again not significant. NAb GMTs between different dose groups of mice varied depending on the dose of the vaccine antigen, with higher dose producing somewhat higher titers. Moreover, starting from the 5th week in BALB/c mice overall NAb GMTs, induced by 6 $\mu\text{g}/\text{dose}$, were significantly higher, than those induced by 1.5 $\mu\text{g}/\text{dose}$ (Mann–Whitney test, $p < 0.05$).

Robustness of the manufacturing process of the vaccine covivac

The robustness of the manufacturing process between different vaccine lots was studied in BALB/c mice. Groups of 10–15 mice were twice immunized with a 14-day period with four different batches of the vaccine CoviVac (InCV-04, -12, -14 and -15, 3–6 $\mu\text{g}/\text{dose}$, 0.5 ml). Blood samples were collected on weeks 2, 3, 5 and 8 after the 1st immunization. Serum samples were analysed individually in NT. As shown in Figure 7, all tested lots induced 100% seroconversion on day 21 with NAb GMTs over 1:32. Some significant differences were observed between NAb levels induced by different vaccine batches 2–3 weeks after the 1st immunization. Nevertheless, antibody titers stabilized on similar levels 5–8 weeks after the 1st immunization without significant differences between the vaccine lots, indicating the robustness of the vaccine production process.

Discussion

Four inactivated vaccines have been approved and are in use in several countries (Table 1). The drastic global shortage of the COVID-19 vaccines and successful clinical trials of the several inactivated preparations make this approach appropriate for inactivated vaccine producers. The Chumakov Center has successfully developed two inactivated vaccines produced in Vero cells against tick-borne encephalitis and poliomyelitis [24, 25]. Therefore, the development of the COVID-19 vaccine was based on the established cell cultivating platform using previously established methods.

Characterization of the vaccine CoviVac

The structure of the production process of the vaccine CoviVac (Figure 1(A)) is rather similar to the ones presented for other inactivated vaccines against COVID-19 [26–28]. Beta-propiolactone was used to shorten the production process. TEM (Figure 1(B)) proved the homogeneity and purity of the vaccine preparation and revealed spiked virions, consistent in shape and size with other studies [28, 29]. Spike structure was consistent with the pre-fusion state of the virions [30]. Resulting vaccine concentrate contained mainly SARS-CoV-2 proteins S and N in detectable amounts, which was supported with Western blot with COVID-19 convalescent serum (Figure 1(C)) and with mouse anti-protein S antibodies (Figure 1(D)). Antibodies induced in mice immunized with CoviVac inactivated vaccine reacted with the native virions produced in Vero cells infected with SARS-CoV-2 clinical isolate, which proves that inactivation process has no significant effect on the antigenic structure (Figure 1(F)). The intracellular staining pattern was consistent with the earlier described localization of N and S proteins in infected cells [31]. The fluorescence had similar localization when the cells were treated with human COVID-19 convalescent

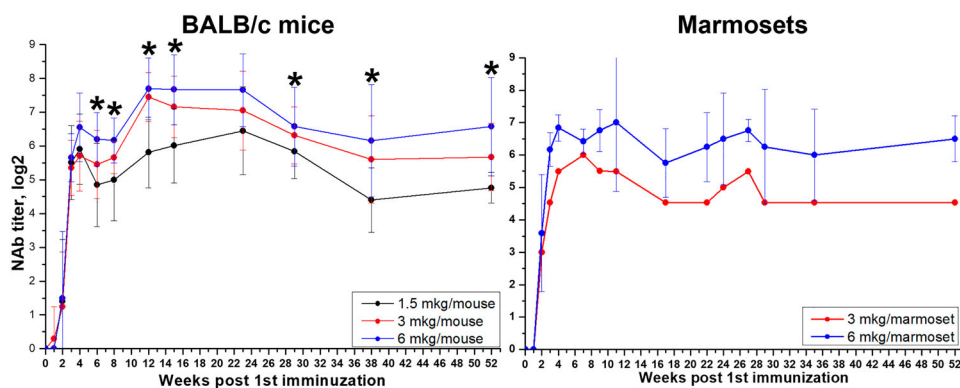


Figure 6. Durability of neutralizing antibody response in BALB/c mice ($N = 20$, 10 animals/group on each time point) and marmosets ($N = 6$ for 6 μg and $N = 1$ for 3 μg) vaccinated with CoviVac (1.5, 3, and 6 μg per dose, 0.5 ml, twice with a 14-day interval) over one year (52 weeks) of observation. *Differences in NAb titers are statistically significant between mice, immunized with 1.5 and 6 μg per dose (Mann–Whitney test, $p < 0.05$).

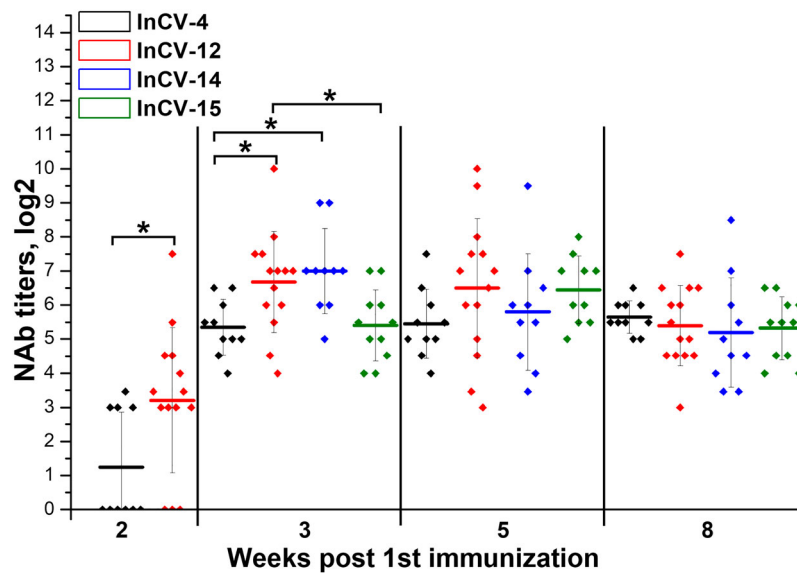


Figure 7 . Immunogenicity of different CoviVac vaccine lots in BALB/c mice (immunized twice with a 14-day interval, nABs were determined 2–8 weeks after the 1st immunization). Line shows mean, whiskers show \pm SD. * Differences are statistically significant (Mann–Whitney test, $p < 0.05$).

Table 1. Inactivated vaccines against COVID-19 approved for use.

Name	Producer	Schedule	Efficacy	Pre-clinical ref	Clinical ref
BBIBP-CorV	Beijing Institute of Biological Products + Sinopharm, China	2 doses, 3 weeks apart	78.1%	27	26
–	Wuhan Institute of Biological Products + Sinopharm, China	2–3 doses, 3–4 weeks apart	72.8%	–	27
CoronaVac (formerly PiCoVacc)	Sinovac Biotech, China	2 doses, 2 weeks apart	50.65–83.5%	25	20
Covaxin (also known as BBV152 A, B, C)	Indian Council of Medical Research + the National Institute of Virology + Bharat Biotech	2 doses, 4 weeks apart	77.8%	24	18

serum (Figure 1(G)), yet the intensity was lower when the mouse serum was used. The specificity of antibody reactivity was confirmed by the absence of fluorescence in non-infected Vero cells (data not shown).

Safety

There are many tests to evaluate various safety parameters of the vaccine candidates in animal models. We chose classical safety animal models of mice, guinea pigs and rats, and non-human primates. For CoviVac we evaluated general acute toxicity in three species (mice, guinea pigs and marmosets), chronic toxicity in two species (mice and guinea pigs), and hypersensitivity in guinea pigs. We did not observe any changes in vaccinated animals in comparison with the placebo groups. All parameters were within physiological norm.

There were some speculations of the possible reproductive toxicity of the vaccine preparations containing SARS-CoV-2 protein S. From our data from experiments involving Wistar rats we can conclude that multiple immunizations with the vaccine CoviVac before or during pregnancy do not have a negative effect on the

prenatal development of the offspring or affect the development of the offspring in the postnatal period.

Therefore, the vaccine CoviVac is safe and can be used in clinical trials in humans.

Immunity and its durability

We evaluated the short-term immunogenicity of the vaccine CoviVac in three animal models (two lines of mice, Syrian hamsters and common marmosets) immunized with different doses. The vaccine induced NABs in all studied species. Moreover, we detected antibodies to both main structural proteins S and N in mice. During the first 2–4 weeks, we did not observe significant differences between NAb titers induced by different doses of the antigen. The differences became significant starting from week 5 post first immunization.

NABs are shown to be one of the main correlates of protection against SARS-CoV-2 [8]. Therefore, the durability of NAb response correlates with the durability of protection. After natural infection, especially

after mild cases, the NAb response is rather low and short [11].

The data on durability of vaccine-induced immunity are very scarce. While there are published preclinical studies demonstrating the induction of total anti-SARS-CoV-2 IgG and NAb by various vaccines, few are focusing on the longevity of the immune response. The data in published preclinical reports on inactivated vaccines against COVID-19 demonstrate the antibody levels after vaccination until week 6 for PiCoVacc in mice and rats and until week 3 for rhesus macaques [27]. In the work published by Wang et al., the immunogenicity analysis in animals was limited to 4 weeks [29]. For BBV152 vaccine candidate, the immunogenicity of the three-dose regimen in hamsters was evaluated until day 25 [32]. We evaluated the long-term immunogenicity in mice and marmosets for one year. We did not observe a significant decrease in NAb titers over this period. Lower doses of the antigen resulted in lower NAb titers over prolonged period of observation. While it is obvious that the decisive data on the long-term immunity provided by the vaccines against COVID-19 will be acquired in longitudinal clinical studies, animal models could serve as helpful surrogate indicators on the earlier stages of the vaccine development process. In a recent clinical report Moderna's mRNA vaccine provided elevated levels of specific antibodies for at least three months [33]. Considering our experimental data, CoviVac vaccine provided a stable long-term immunity upon course of two vaccination in mice and marmosets.

Protective efficacy

Many recent studies describe the golden (Syrian) hamster model of SARS-CoV-2 infection as a consistent and valid non-lethal small animal model for studying the protective efficacy of vaccines against COVID-19. SARS-CoV-2 infection of Syrian hamsters can cause significant pathological changes in lungs of infected hamsters and support the development of stable post-infection humoral immune response in passive transfer experiments [33]. Moreover, the observed immunohistochemical changes and weight loss patterns in hamsters resemble the course of mild SARS-CoV-2 infection in humans [34]. A number of works showed the validity of Syrian hamster model to be used for studies of protective efficacy of NAb and vaccines against SARS-CoV-2 [35–44], although the pneumonia signs were fast developing and severe.

Syrian hamster model was used to evaluate the protective efficacy of several inactivated vaccines [45–46], including ones certified for clinical use [31]. The main evaluated parameters were weight, virus and/or viral RNA presence in nasal swabs, lungs and other organs

on different terms post infection. We chose the same parameters for our experiments.

In our study, control animals lost weight till 5–7 d p.i., whereas vaccinated ones gained weight starting from day 3 p.i., which was comparable to the data for BBV152 [31]. However, weight loss by control animals in our experiments was more pronounced, 15% vs. 2–10%. The rates of upper respiratory tract clearance of viral RNA were similar as well: starting from day 7 p.i. most of the nasal swabs did not contain viral RNA. Viral RNA detection in lungs of control animals was similar in both studies; in our experiments, the organs of all investigated control animals contained viral RNA on days 4, 7 and 14 p.i. Lung tissues of vaccinated animals were mostly cleared of the virus: only 1 of 5 animals had detectable RNA levels in lungs on days 4 and 7 p.i., that were cleared by day 14. Viral RNA was detected in extra-pulmonary tissues of control animals only 3 days p.i. Similar results were obtained for BBV152 [31]. Therefore, the data demonstrated the protective efficacy of CoviVac in hamster model.

In conclusion, the vaccine CoviVac showed no signs of acute/chronic, reproductive, embryo- and fetotoxicity, or teratogenic effects in the antenatal and postnatal periods of development, as well as no allergenic properties in studied animal species. The vaccine produced stable and robust humoral immune response both in form of specific anti-SARS-CoV-2 IgG and NAb in rodents and non-human primates. The NAb levels did not decrease significantly over the course of one year. CoviVac showed protective effect against SARS-CoV-2 infection in Syrian hamsters. Robustness of the vaccine manufacturing process was demonstrated. These data encouraged further evaluation of CoviVac in clinical trials.

Acknowledgements

OSS, MPK and KVS acknowledge support from the Interdisciplinary Scientific and Educational School of Moscow Lomonosov University “Molecular Technologies of the Living Systems and Synthetic Biology.” Electron microscopy was performed using the Unique equipment setup “3D-EMC” of Moscow State University, Faculty of Biology. Confocal microscopy was made using the equipment located at the User Facilities Center of Moscow State University, including the equipment purchased on account of the MSU Development Program to 2020.

Disclosure statement

Most of the authors work for Chumakov FSC R&D IBP RAS - CoviVac developer and producer.

Funding

The work was partially supported by Ministry of Science and Higher Education of the Russian Federation, AAAA-A20-120081790043-5, and RFBR grant 20-04-60258.

Author contributions

LIK, ANP, GMI, IVG, KMM, OSG, LVG, EGI, ASS: conceptualization, LIK, ANP, GMI, IVG, AAS, AAK, KMM, OSG, OSS, LVG, EGI, ASS: methodology, LIK, GMI, IVG, LVG: formal analysis, LIK, ANP, GMI, IVG, VPV, YVR, AAS, AAK, YYI, LPA, KMM, LSP, ASS, YYT, EOB, OSG, VVI, GSG, OSS, AMM, SAG, TVG, AVM, LVG, EGI: investigation, LIK and VPV: writing – original draft; LIK, IVG and all authors: writing – review and editing; LIK, IVG, AAS, OSS, AMM: visualization; LIK, ANP, GMI, IVG, AAK, LVG, EGI, ASS: supervision; LIK, ANP, GMI, IVG, LVG, EGI, MPK, AME, ASS, AAI: project administration; AAI: funding acquisition.

ORCID

Liubov I. Kozlovskaya  <http://orcid.org/0000-0002-3029-1035>

Viktor P. Volok  <http://orcid.org/0000-0002-9659-723X>

Aydar A. Ishmukhametov  <http://orcid.org/0000-0001-6130-4145>

References

- [1] WHO COVID-19 Dashboard [Internet]. Geneva: World Health Organization; 2020 [cited 2021 Aug 12]. Available from: <https://covid19.who.int/>.
- [2] COVID-19 Dashboard by the Center for Systems Science and Engineering (CSSE) at Johns Hopkins University (JHU) [Internet]. [cited 2021 Mar 27]. Available from: <https://gisanddata.maps.arcgis.com/apps/opsdashboard/index.html#/bda7594740fd40299423467b48e9ecf6>.
- [3] International Committee on Taxonomy of Viruses (ICTV) [Internet]. [cited 2021 Mar 14]. Available from: <https://ictv.global/taxonomy/>.
- [4] Hoffmann M, Kleine-Weber H, Schroeder S, et al. SARS-CoV-2 cell entry depends on ACE2 and TMPRSS2 and is blocked by a clinically proven protease inhibitor. *Cell*. 2020;181(2):271–280.e8.
- [5] Zhou P, Yang XL, Wang XG, et al. A pneumonia outbreak associated with a new coronavirus of probable bat origin. *Nature*. 2020 Mar;579(7798):270–273.
- [6] Cai Y, Zhang J, Xiao T, et al. Distinct conformational states of SARS-CoV-2 spike protein. *Science*. 2020;369(6511):1586–1592.
- [7] Walls AC, Park YJ, Tortorici MA, et al. Structure, function, and antigenicity of the SARS-CoV-2 spike glycoprotein. *Cell*. 2020 Apr 16;181(2):281–292.e6. Erratum in: *Cell*. 2020;183(6):1735.
- [8] McMahan K, Yu J, Mercado NB, et al. Correlates of protection against SARS-CoV-2 in rhesus macaques. *Nature*. 2021;590(7847):630–634.
- [9] Seow J, Graham C, Merrick B, et al. Longitudinal observation and decline of neutralizing antibody responses in the three months following SARS-CoV-2 infection in humans. *Nat Microbiol*. 2020;5(12):1598–1607.
- [10] Wang K, Long QX, Deng HJ, et al. Longitudinal dynamics of the neutralizing antibody response to SARS-CoV-2 infection. *Clin Infect Dis*. 2021;73(3):e531–e539.
- [11] Wajnberg A, Amanat F, Firpo A, et al. Robust neutralizing antibodies to SARS-CoV-2 infection persist for months. *Science*. 2020;370(6521):1227–1230.
- [12] Shrotri M, Swinnen T, Kampmann B, et al. An interactive website tracking COVID-19 vaccine development. *Lancet Glob Health*. 2021;9(5):e590–e592.
- [13] Baden LR, El Sahly HM, Essink B, et al. Efficacy and safety of the mRNA-1273 SARS-CoV-2 vaccine. *N Engl J Med*. 2021;384(5):403–416.
- [14] Logunov DY, Dolzhikova IV, Shcheblyakov DV, et al. Safety and efficacy of an rAd26 and rAd5 vector-based heterologous prime-boost COVID-19 vaccine: an interim analysis of a randomised controlled phase 3 trial in russia. *Lancet*. 2021;397(10275):671–681. Erratum in: *Lancet*. 2021;397(10275):670.
- [15] Bandyopadhyay AS, Garon J, Seib K, et al. Polio vaccination: past, present and future. *Future Microbiol*. 2015;10(5):791–808.
- [16] Demicheli V, Jefferson T, Ferroni E, et al. Vaccines for preventing influenza in healthy adults. *Cochrane Database Syst Rev*. 2018;2(2):CD001269.
- [17] Che Y, Liu X, Pu Y, et al. Randomized, double-blinded and placebo-controlled phase II trial of an inactivated SARS-CoV-2 vaccine in healthy adults. *Clin Infect Dis*. 2020: ciaa1703. doi:10.1093/cid/ciaa1703.
- [18] Ella R, Reddy S, Jogdand H, et al. Safety and immunogenicity of an inactivated SARS-CoV-2 vaccine, BBV152: interim results from a double-blind, randomised, multicentre, phase 2 trial, and 3-month follow-up of a double-blind, randomised phase 1 trial. *Lancet Infect Dis*. 2021;S1473-3099(21):00070-0.
- [19] Wu Z, Hu Y, Xu M, et al. Safety, tolerability, and immunogenicity of an inactivated SARS-CoV-2 vaccine (CoronaVac) in healthy adults aged 60 years and older: a randomised, double-blind, placebo-controlled, phase 1/2 clinical trial. *Lancet Infect Dis*. 2021;S1473-3099 (20):30987-7.
- [20] Zhang Y, Zeng G, Pan H, et al. Safety, tolerability, and immunogenicity of an inactivated SARS-CoV-2 vaccine in healthy adults aged 18-59 years: a randomised, double-blind, placebo-controlled, phase 1/2 clinical trial. *Lancet Infect Dis*. 2021;21(2):181–192.
- [21] Wang H, Zhang Y, Huang B, et al. Development of an inactivated vaccine candidate, BBIBP-CorV, with potent protection against SARS-CoV-2. *Cell*. 2020;182(3):713–721.e9.
- [22] Zhang J, Cruz-Cosme R, Zhuang MW, et al. A systemic and molecular study of subcellular localization of SARS-CoV-2 proteins. *Signal Transduct Target Ther*. 2020;5(1):269.
- [23] Kärber G. Beitrag zur kollektiven behandlung pharmakologischer reihenversuche. *Archiv f Experiment. Pathol u Pharmakol*. 1931;162:480–483. DOI:10.1007/BF01863914.
- [24] Scudiero DA, Shoemaker RH, Paull KD, et al. Evaluation of a soluble tetrazolium/formazan assay for cell growth and drug sensitivity in culture using human and other tumor cell lines. *Cancer Res*. 1988;48(17):4827–4833.
- [25] Kozlovskaya L, Piniavaeva A, Ignatyev G, et al. Isolation and phylogenetic analysis of SARS-CoV-2 variants collected in Russia during the COVID-19 outbreak. *Int J Infect Dis*. 2020;99:40–46. Erratum in: *Int J Infect Dis*. 2021;103:644.
- [26] Vorovitch MF, Grishina KG, Volok VP, et al. Evervac: phase I/II study of immunogenicity and safety of a new adjuvant-free TBE vaccine cultivated in Vero cell culture. *Hum Vaccin Immunother*. 2020;16(9):2123–2130.

- [27] Pinaeva A, Ivin Y, Kovpak A, et al. Inactivated polio vaccine based on Sabin strains. Proceedings of the International Conference on Perspective Technologies in Vaccination and Immunotherapy. 2020 Oct 27–29. Moscow, Russia. ISSN 2619-1121. Available from: <http://techvac.org/wp-content/uploads/2020/12/Abstract-Book-TECHVAC2020-final-1.pdf>.
- [28] Xia S, Zhang Y, Wang Y, et al. Safety and immunogenicity of an inactivated SARS-CoV-2 vaccine, BBIBP-CorV: a randomised, double-blind, placebo-controlled, phase 1/2 trial. safety and immunogenicity of an inactivated SARS-CoV-2 vaccine, BBIBP-CorV: a randomised, double-blind, placebo-controlled, phase 1/2 trial. *Lancet Infect Dis*. 2021;21(1):39–51.
- [29] Xia S, Duan K, Zhang Y, et al. Effect of an inactivated vaccine against SARS-CoV-2 on safety and immunogenicity outcomes: interim analysis of 2 randomized clinical trials. *JAMA*. 2020;324(10):951–960.
- [30] Bagrov DV, Gluhov GS, Moiseenko AV, et al. Structural Characterization of β -Propiolactone Inactivated SARS-CoV-2 Particles. *Microsc Res Tech*. doi:10.1002/jemt.23931.
- [31] Ganneru B, Jogdand H, Daram VK, et al. Evaluation of Safety and Immunogenicity of an Adjuvanted, TH-1 Skewed, Whole Virion Inactivated SARS-CoV-2 Vaccine - BBV152. 2020 [cited 14 Mar 2021]. Available from: <https://ssrn.com/abstract=3737812>.
- [32] Mohandas S, Yadav PD, Shete A, et al. Immunogenicity and protective efficacy of BBV152, whole virion inactivated SARS-CoV-2 vaccine candidates in the Syrian hamster model. *iScience*. 2021;24(2):102054.
- [33] Widge AT, Roupheal NG, Jackson LA, et al. Durability of responses after SARS-CoV-2 mRNA-1273 vaccination. *N Engl J Med*. 2021;384(1):80–82.
- [34] Gao Q, Bao L, Mao H, et al. Development of an inactivated vaccine candidate for SARS-CoV-2. *Science*. 2020;369(6499):77–81.
- [35] Wang ZJ, Zhang HJ, Lu J, et al. Low toxicity and high immunogenicity of an inactivated vaccine candidate against COVID-19 in different animal models. *Emerg Microbes Infect*. 2020;9(1):2606–2618.
- [36] Imai M, Iwatsuki-Horimoto K, Hatta M, et al. Syrian hamsters as a small animal model for SARS-CoV-2 infection and countermeasure development. *Proc Natl Acad Sci U S A*. 2020;117(28):16587–16595.
- [37] Sia SF, Yan LM, Chin AWH, et al. Pathogenesis and transmission of SARS-CoV-2 in golden hamsters. *Nature*. 2020;583(7818):834–838.
- [38] Rogers TF, Zhao F, Huang D, et al. Isolation of potent SARS-CoV-2 neutralizing antibodies and protection from disease in a small animal model. *Science*. 2020;369(6506):956–963.
- [39] Tostanoski LH, Wegmann F, Martinot AJ, et al. Ad26 vaccine protects against SARS-CoV-2 severe clinical disease in hamsters. *Nat Med*. 2020;26(11):1694–1700.
- [40] Kuo TY, Lin MY, Coffman RL, et al. Development of CpG-adjuvanted stable prefusion SARS-CoV-2 spike antigen as a subunit vaccine against COVID-19. *Sci Rep*. 2020;10(1):20085.
- [41] Sun W, McCroskery S, Liu WC, et al. A newcastle disease virus (NDV) expressing a membrane-anchored spike as a cost-effective inactivated SARS-CoV-2 vaccine. *Vaccines (Basel)*. 2020;8(4):771.
- [42] Yahalom-Ronen Y, Tamir H, Melamed S, et al. A single dose of recombinant VSV- Δ G-spike vaccine provides protection against SARS-CoV-2 challenge. *Nat Commun*. 2020;11(1):6402.
- [43] Hörner C, Schürmann C, Auste A, et al. A highly immunogenic and effective measles virus-based Th1-biased COVID-19 vaccine. *Proc Natl Acad Sci U S A*. 2020;117(51):32657–32666.
- [44] Rauch S, Roth N, Schwendt K, et al. mRNA-based SARS-CoV-2 vaccine candidate CVnCoV induces high levels of virus-neutralising antibodies and mediates protection in rodents. *NPJ Vaccines*. 2021;6(1):57.
- [45] Li M, Guo J, Lu S, et al. Single-Dose immunization With a chimpanzee adenovirus-based vaccine induces sustained and protective immunity against SARS-CoV-2 infection. *Front Immunol*. 2021;12:697074.
- [46] Kalnin KV, Plitnik T, Kishko M, et al. Immunogenicity and efficacy of mRNA COVID-19 vaccine MRT5500 in preclinical animal models. *NPJ Vaccines*. 2021;6(1):61.
- [47] Bricker TL, Darling TL, Hassan AO, et al. A single intranasal or intramuscular immunization with chimpanzee adenovirus-vectored SARS-CoV-2 vaccine protects against pneumonia in hamsters. *Cell Rep*. 2021 Jul 20;36(3):109400.
- [48] Kandeil A, Mostafa A, Hegazy RR, et al. Immunogenicity and safety of an inactivated SARS-CoV-2 vaccine: preclinical studies. *Vaccines (Basel)*. 2021;9(3):214.
- [49] Ragan IK, Hartson LM, Dutt TS, et al. A whole virion vaccine for COVID-19 produced via a novel inactivation method and preliminary demonstration of efficacy in an animal challenge model. *Vaccines (Basel)*. 2021;9(4):340.